Audio Engineering Society

Convention Paper

Presented at the 129th Convention
2010 November 4–7 San Francisco, CA, USA

Optimal Location and Orientation for Midrange and High Frequency Loudspeakers in the Instrument Panel of an Automotive Interior

Roger Shively[1], Jérôme Halley[2], François Malbos[3], and Gabriel Ruiz[4]

[1] Harman International, Novi, Michigan, USA
Roger.Shively@harman.com

[2] Harman International, Karlsbad, Germany
Jerome.Halley@harman.com

[3] Harman International, Chateau du Loir, France
Francois.Malbos@harman.com

[4] Harman International, Bridgend, Wales, UK
Gabriel.Ruiz@harman.com

ABSTRACT

In a follow-up to a previous paper (AES Preprint 8023, May 2010) [1] using the modeling process described there for modeling loudspeakers in an automotive interior, the optimization of midrange and of high frequency tweeter loudspeakers' positions for best acoustic performance in the driver's side (left) and passenger's side (right) of automotive instrument panel is reported on.

1. INTRODUCTION

In the previous paper [1], we began the first step in a study to determine the validity of some best practice guidelines for the positioning of instrument panel midranges and to set the stage for making the analysis of such complex sound fields common place. [2] [Also see Appendix § 8.1]

In that paper the framework of the process used to obtain an accurate model of the vehicle interior and to show early results from the models was demonstrated.

The geometry for the vehicle interior comes from CATIA CAD data; in this case, it has been that of a sedan vehicle. That data is the basis of the acoustic mesh. There are two acoustic solution techniques that are used. The lower frequency part of the frequency response in the simulation result is calculated by a wave expansion technique and the upper frequency part by a ray launching algorithm.

The first model uses characteristic boundary conditions, with no model updates. The second model is derived from a model update procedure for low- and high-frequencies that involves the results from the first model and measured data from the vehicle. This process is described in the Appendices (§§ 8.2-8.4) of this paper and in more detail in the previous paper. [1]

The larger scope of the study is to find optimal locations for midranges and tweeters in instrument panels, doors, rear decks, and any of the pillar locations available in the automotive interior. For the instrument panel, the locations of interest are the left, right, and center. Previously, to test the validity of the process, we began with a simulation of a loudspeaker in the center channel location on the instrument panel and a simple optimization of its location and angle of orientation.

In this paper we continue that work. We applied the process to outboard, left and right, midrange loudspeakers to determine the optimal location on the instrument panel with respect to the near boundaries and with respect to the angle the plane of the loudspeaker makes relative to the surface of the instrument panel. In addition, we investigated the optimal location of a tweeter location for and around the center channel loudspeaker. We begin with the left and right outboard midranges.

Figure 1 shows the location of the left and right midrange loudspeakers in the instrument panel. And Figure 2 shows an example of the mesh created for the loudspeakers and the instrument panel (IP).

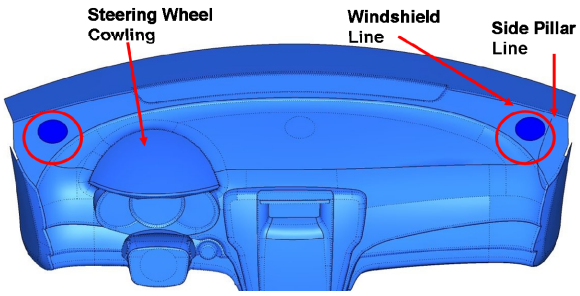

Figure 1. Left and Right Instrument Panel Midragne Loudspeaker Locations (Config 9 & 24).

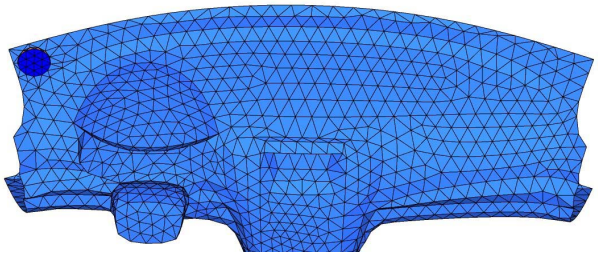

Figure 2. IP Acoustic Mesh with Left Loudspeaker location. (Config 9)

2. COMBINED MODELS (OUTBOARD MIDRANGES)

2.1. Investigated Midrange Loudspeaker Locations and Angles

The location of the left midrange is shown in Figure 3. The Blue position is considered the reference (Config 9) It is located as close as possible to any surface created by the corner of the side pillar and the windshield. All the other positions are created and investigated with reference to it. Figures 4, 5, and 6 show the angles relative to the Blue reference position and relative to the surface of the IP.

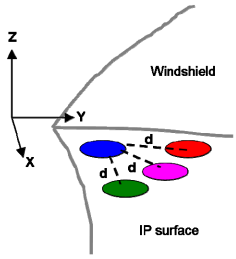

LEFT OUTBOARD MID					
CFG	T	θ (º)	Φ (º)	Ω (º)	
9	0	α	0	0	○
10	0	α	+10	0	□
11	0	α	-10	0	×
15	d	α	0	0	○
16	d	α	+10	0	□
17	d	α	-10	0	×
18	d	α+90	0	0	○
19	d	α+90	0	+10	□
20	d	α+90	0	-10	×
21	d	α+45	0	0	○
22	d	α+45	+10	0	□
23	d	α+45	-10	0	×

Figure 3. Left IP Midrange Positions and Angles. Blue is the reference position, located 1 cm away from any corner of the side pillar or windshield. d = the midrange diameter. α = the smallest angle so the Green position is located 1 cm away from the side pillar.

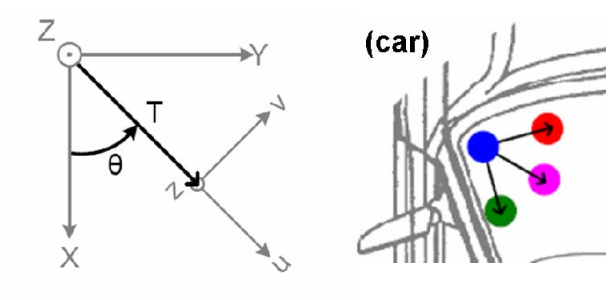

Figure 4. T is the translation vector in the global coordinates xyz. θ is the oriented angle about the Z-axis.

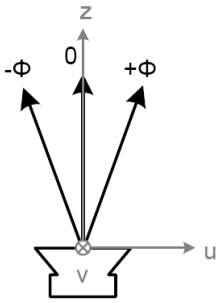

Figure 5. Local coordinates uvz. Φ is the oriented angel about the V-axis.

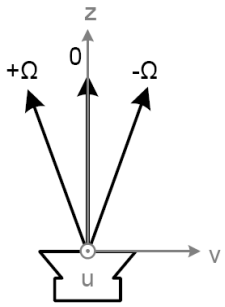

Figure 6. Local coordinates uvz. Ω is the oriented angle about the U-axis.

The right IP loudspeaker positions and angles follow the same conventions as for the left. It's configurations are listed in Figure 7.

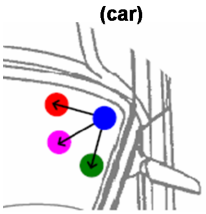

RIGHT OUTBOARD MID					
CFG	T	θ (º)	Φ (º)	Ω (º)	
24	0	-α	0	0	○
25	0	-α	+10	0	□
26	0	-α	-10	0	×
27	d	-α	0	0	○
28	d	-α	+10	0	□
29	d	-α	-10	0	×
30	d	-α-90	0	0	○
31	d	-α-90	0	-10	□
32	d	-α-90	0	+10	×
33	d	-α-45	0	0	○
34	d	-α-45	+10	0	□
35	d	-α-45	-10	0	×

Figure 7. Right IP Midrange Positions and Angles.

The anechoic data for the midrange that was to be modeled as the source is shown in Figure 8.

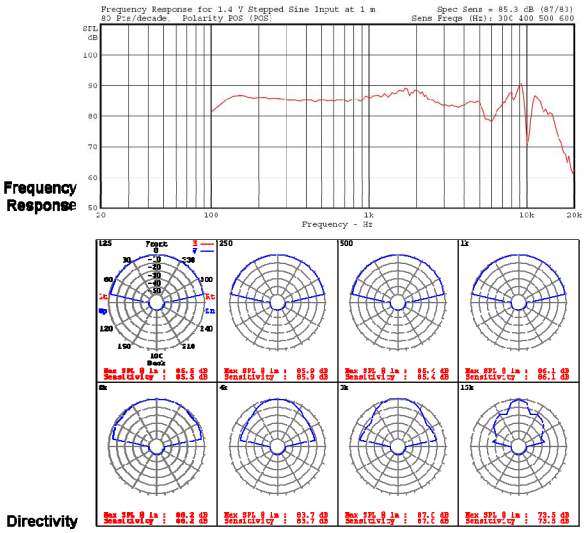

Figure 8. On-Axis Anechoic Frequency Response and Directivity of the Source.

2.2. Low-Frequency Model Results

Low-frequency modeling was based on a full domain discretization approach. The cabin volume was meshed with tetrahedral elements and a solution was found by numerically approximating the steady-state Helmholtz equation at each mesh point.

The solution thus obtained assumes transient effects have vanished. The acoustic field at each mesh point then varies harmonically with time.

To obtain a numerical approximation of the acoustic field, several techniques may be used. For this project, a highly accurate wave expansion approach – several times more efficient than commercially available tools – was implemented.

Some example results from the low-frequency model of the left and right IP midranges are shown in Figures 9 a, b.

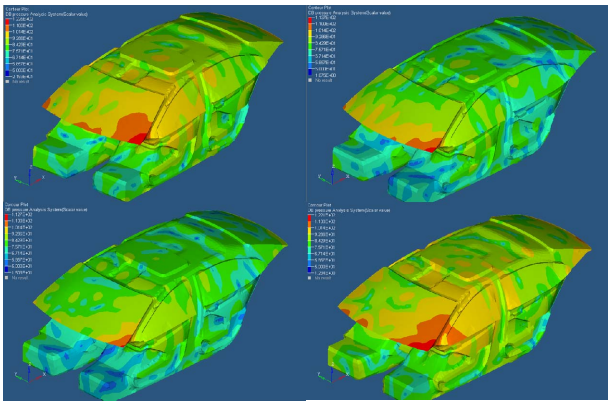

Figure 9a. **Left** Midrange Low-Frequency Model Result at 750Hz for: Config 9, 15, 18, and 21. (clockwise).

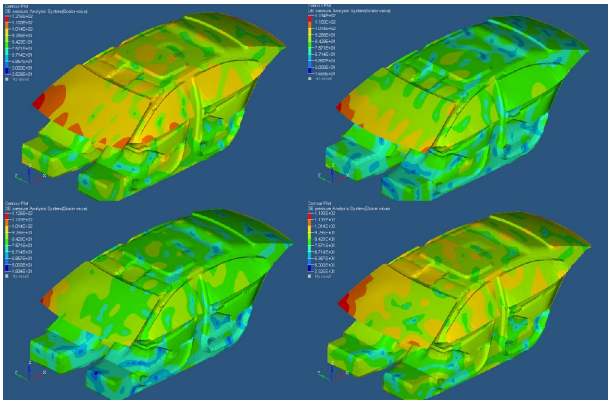

Figure 9b. **Right** Midrange Low-Frequency Model Result at 750Hz for: Config 24, 27, 30, and 33. (clockwise).

2.3. High-Frequency Model Results

The high-frequency model utilizes a simulation technique based on Geometrical Acoustics (GA). [See Appendix § 8.5]

An example of the Rays launch results is given in Figure 10 a, b, and c for 4kHz. We can see how the wavefronts from the loudspeaker and its initial reflection(s) combine at the listening positions.

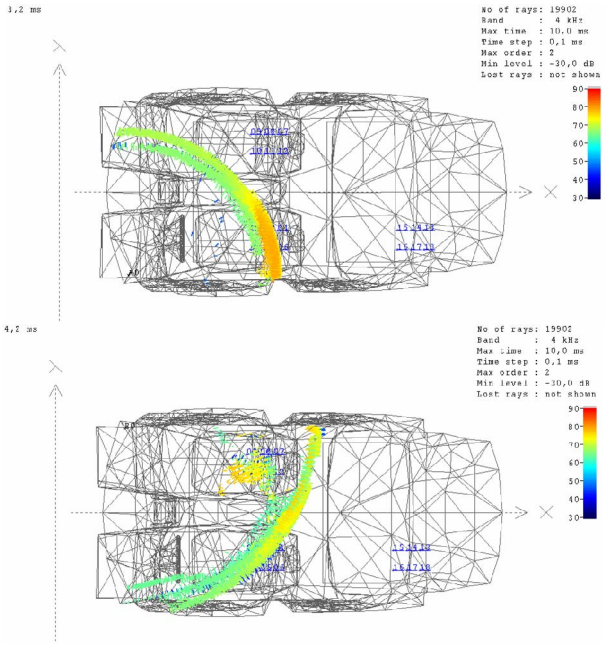

Figure 10a. High-Frequency Model Result for 4kHz of Left Config 9 (top) and Right Config 24 (bottom) @ **Array A**

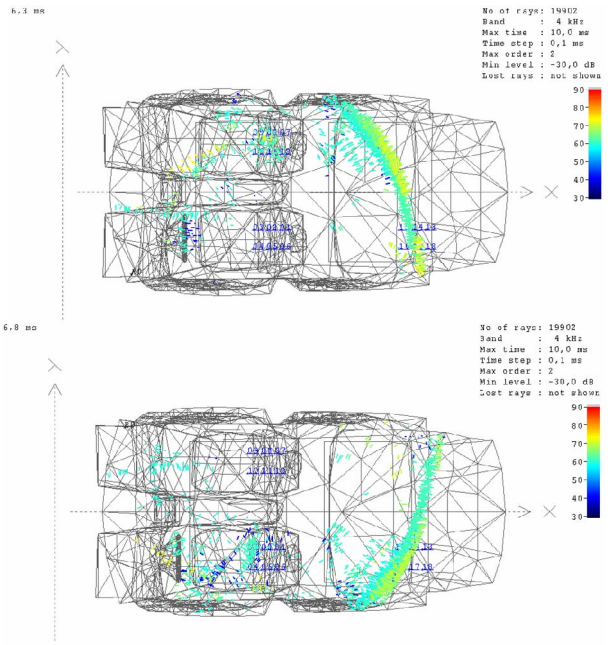

Figure 10c. High-Frequency Model Result for 4kHz of Left Config 9 (top) and Right Config 24 (bottom) @ **Array C**

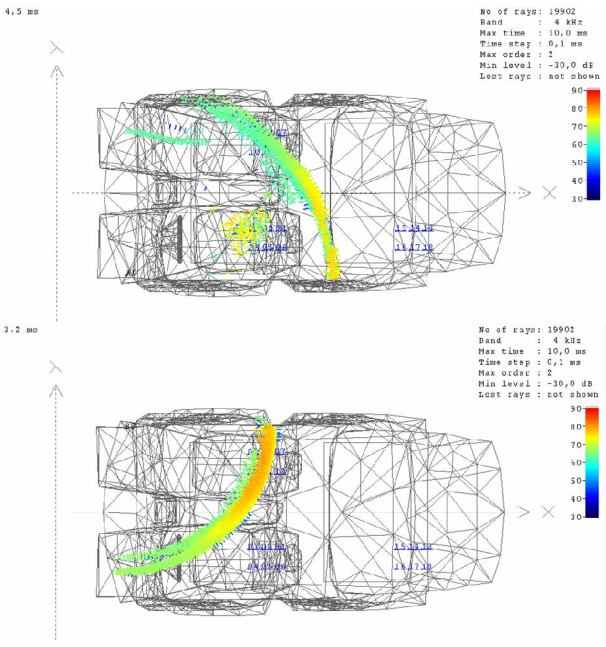

Figure 10b. High-Frequency Model Result for 4kHz of Left Config 9 (top) and Right Config 24 (bottom) @ **Array B**

3. COMBINED (LF & HF) OUTBOARD MIDRANGE RESULTS

The combined low frequency and high frequency results [Figures 12, 13, 14, 15, 16, 17] are shown as typical SPL response versus microphone location. The microphone locations (Array's A, B, and C) are those that would be measured in an automotive interior. These locations are shown in Figure 11.

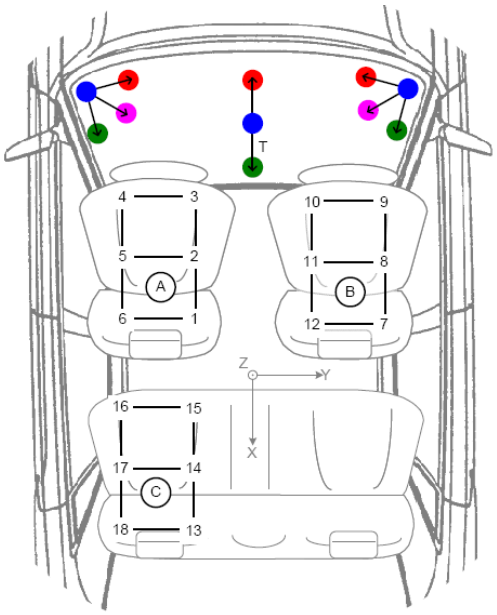

Figure 11. Microphone Array Positions A, B, and C for Simulation Results.

The proximity of the midrange loudspeaker to the corner created by the windshield, nearby window pillar, and the IP surface can be seen quite easily in either the mid-band and upper mid-band (400 – 2k Hz) reinforcement or lack of reinforcement depending on location. And, the influence that the cowling hump around the steering wheel has on the upper frequency response can be seen in these results, where it causes the left and right response amplitudes to be asymmetric. The frequency range of the influence is ~3k – 6k Hz. These are common experiences in automotive sound design, which are illustrated nicely here.

As with the center channel midrange from the previous work, the low frequency frequency-step animations give a full understanding of the sound pressure distribution throughout the vehicle at frequencies below 1 kHz. As well, in the high frequency time-step animation of the non-optimal loudspeaker configuration and the optimal configuration, it is easy to see the non-uniformity of the sound propagation and numerous reflections influencing that sound field. It is the non-uniformity that is key to understanding the optimal location. The influence of the loudspeakers location and the boundary conditions is seen in the reflections.

It is even more interesting in the work presented here. The frequency response curves illustrate the combined direct and reflected wavefront amplitudes for both the LF and HF soundfields. The steering wheel cowling improves the performance of the left midrange for the near-side, driver's listening position, and degrades it for all the other positions. Also demonstrated is how the midrange being in a location along the windshield line (both the Blue and the Red locations) displays the benefit of a near boundary to reinforce the mid-band and upper mid-band output, but only for the near-side listener: left speaker for the left listener and right speaker for the right listener.

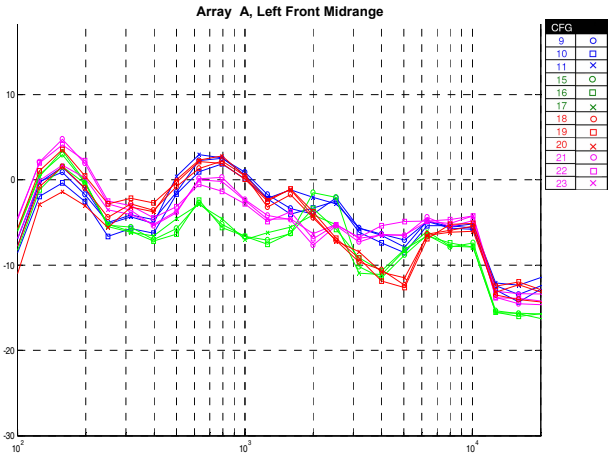

Figure 12. **Left** IP Midrange Concatenated Frequency Responses at Array Position (**A**) Front Driver

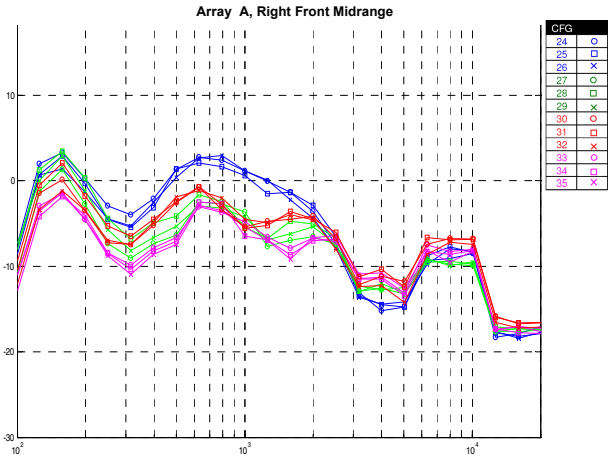

Figure 13. **Right** IP Midrange Concatenated Frequency Responses at Array Position (**A**) Front Driver

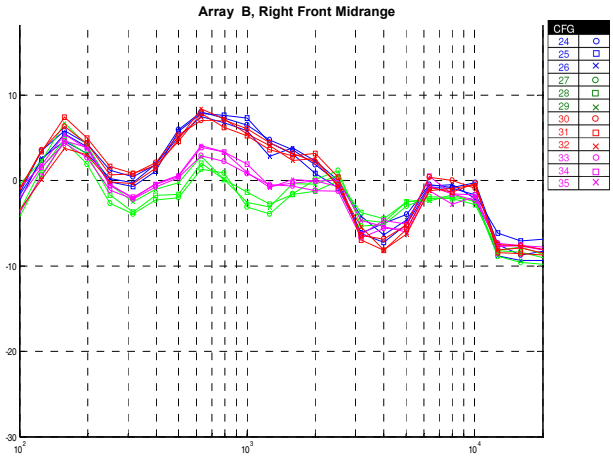

Figure 15. **Right** IP Midrange Concatenated Frequency Responses at Array Position (**B**) Front Passenger

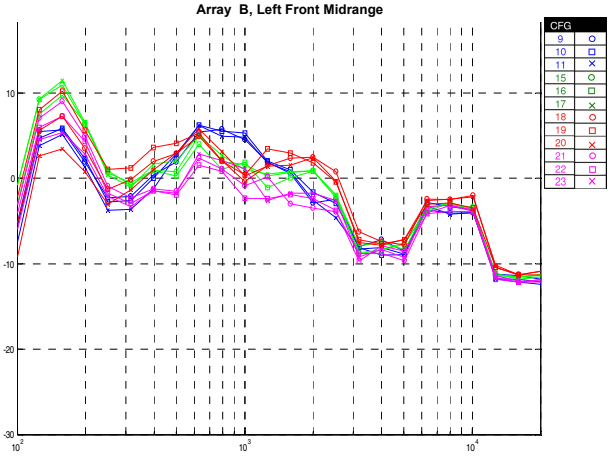

Figure 14. **Left** IP Midrange Concatenated Frequency Responses at Array Position (**B**) Front Passenger

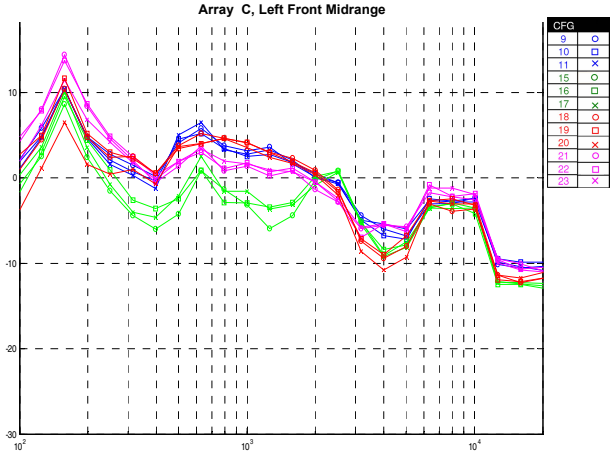

Figure 16. **Left** IP Midrange Concatenated Frequency Responses at Array Position (**C**) Left Rear Seat

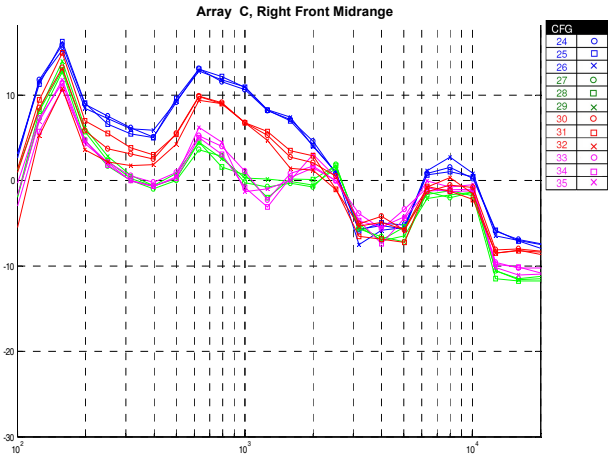

Figure 17. **Right** IP Midrange Concatenated Frequency Responses at Array Position (**C**) Left Rear Seat

CTR TWE				
CFG	T	θ (º)	Φ (º)	
0	d	0	0	○
1	d	0	-α	□
2	d	0	α	×
3	d	0	β	▽
4	d	90	0	○
5	d	90	-α	□
6	d	90	α	×
7	d	90	β	▽
8	d	180	0	○
9	d	180	-α	□
10	d	180	α	×
11	d	180	β	▽
12	d	-90	0	○
13	d	-90	-α	□
14	d	-90	α	×
15	d	-90	β	▽

Figure 18a. Center Tweeter Positions and Angle configurations. d = the distance between tweeter and midrange. d is kept as small as packaging allows. T, θ, and Φ same as Figures 4 & 5.

4. CENTER CHANNEL TWEETER

4.1. Investigated Center Tweeter Locations and Angles

Next we focus on a tweeter positioned near the center channel midrange in the IP. We used the optimal center midrange location from the previous paper as the midrange reference point. The tweeter positions to be investigated were located in four positions around the midrange. The first configuration for each of positions was with the tweeter flush to the IP surface. For the other configurations, the angling of the tweeter relative to the IP surface was investigated for two different goals. First, (the β angle, Point E, in Figure 18b) the tweeter was aimed so that the first reflections would coincide at the driver's head. And second, (the α angle, Pont F, in Figure 18b) the tweeter was aimed so that it was coincident on the windshield with the point where the main axis of the midrange would be if projected on the windshield. One other angle configuration was used, and that was with the tweeter angled away from the midrange by negative α. With the exception of the tweeter being co-axially mounted on the midrange, these are typically all the options that can exist when packaging a tweeter with a center channel midrange. The distance between the tweeter and the midrange was kept as small as possibly allowed. Figure 18a lists the different configurations.

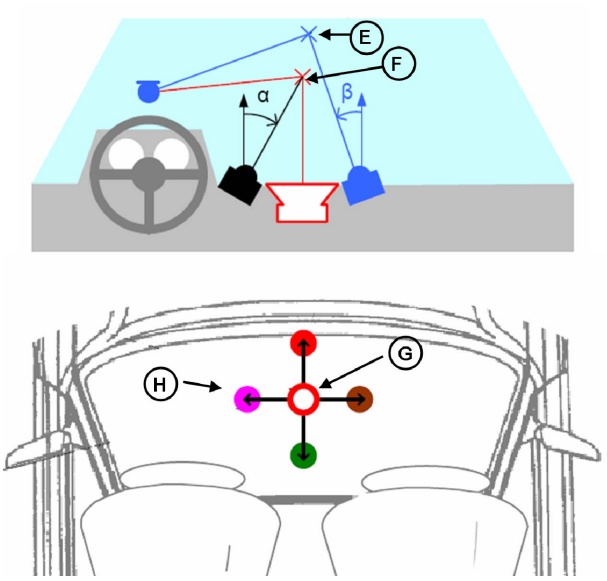

Figure 18b. Center Tweeter Positions and Angle configurations. Point E, β angle, tweeter aimed so 1st reflections coincide @ driver's head. Point F, α angle, main axis coincident point on the windshield. G, optimum mid config from IP mids simulation results. H, 4 tweeter positions simulated.

The anechoic data for the tweeter that was modeled as the source is shown in Figure 19.

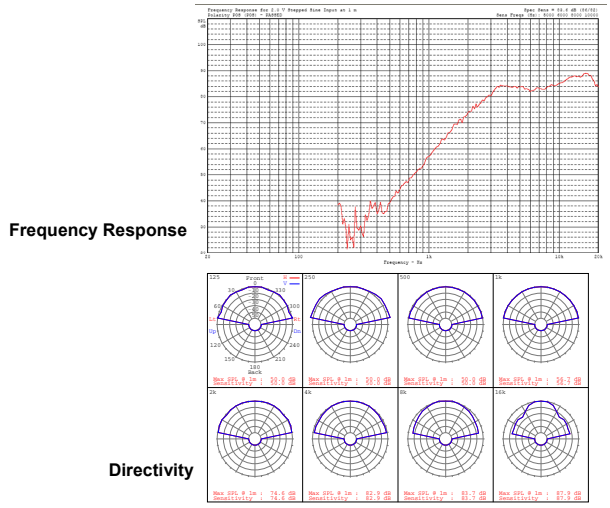

Figure 19. Frequency Response and Directivity of tweeter used as source.

4.2. High Frequency Model Results

We can see that there can be different advantages for each listening position depending which tweeter location and which aiming angle is used. In practice, when the ideal location and solution isn't possible due to vehicle design requirements, then the driver's listening location is usually prioritized above the front seat passenger, with the rear seat passenger prioritized last.

For the driver's listening position, Array A, the ideal configuration for the most output and smoothest response was the Green location, using the β angle. The other most preferred was the Red location, with a negative α angle. The Green location is closest to the edge of the IP. The β angle fires it back into the window. The Red location is at the apex of the windshield and the IP, and the negative α angle fires it toward the windshield. These locations may not be as practical as either the Pink (driver near-side) or Brown (driver far-side) locations. Considering those two locations, the driver near-side location of Pink with a β angle was slightly preferred for its additional output above 10kHz. The driver far-side location of Brown was best with the β angle also.

For the passenger listening position, Array B, the Brown location was least preferred and the Green location most preferred for output and smoothness. Green with a β angle was best. For the Red and Pink locations, α angles provided the best response.

For the left rear passenger listening position, Array C, the Pink location was obscured by the driver's seat, and had the least to recommend it. Location Green flush mounted or with a β angle and Red with a β or α angle were the best for the rear seat. Read flush mounted or Green with an α angle were much less preferred.

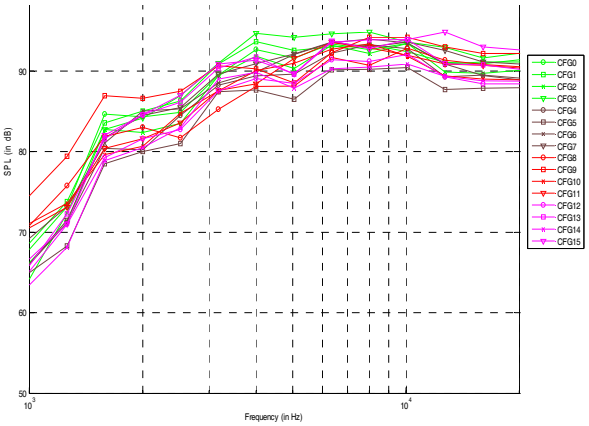

Figure 20. Center Tweeter Frequency Responses at Array Position (**A**) Front Driver

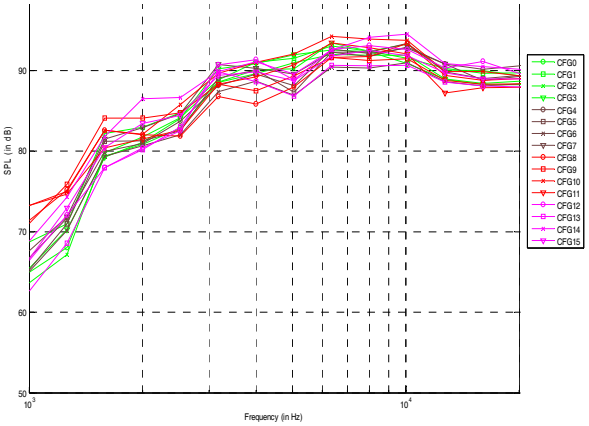

Figure 21. Center Tweeter Frequency Responses at Array Position (**B**) Front Passenger

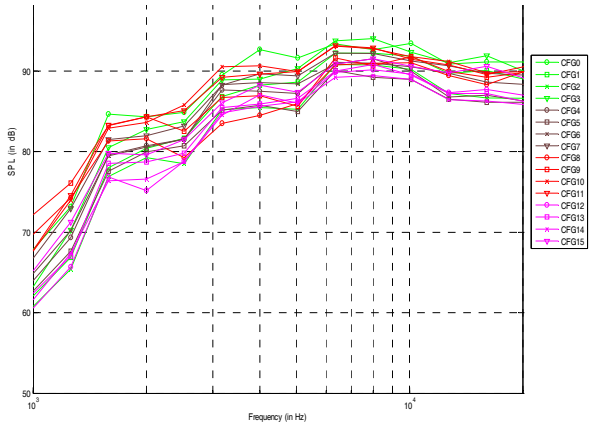

Figure 22. Center Tweeter Frequency Responses at Array Position (**C**) Left Rear Seat

5. CONCLUSIONS

The general conclusions from the combined low frequency and high frequency SPL results are that they are consistent with our common experience. For this specific IP geometry, we can draw the following conclusions.

OUTBOARD MIDRANGES:

- For the listener in the front seat sitting closest to the outboard position in question, the Blue and Red locations show the best mid-band and upper mid-band (400 – 2k Hz) reinforcement.
- The driver side front passenger benefits additionally from the reinforcement of the steering wheel cowling in the 3k – 6k Hz range for the Left Blue and Pink locations.
- In all other listening locations in the vehicle for both the Left speaker and the Right speaker there is a lack of reinforcement in that range.

The location of the midrange located as far as possible into the corner created by the windshield and IP surfaces (Blue) allows for the best reinforcement and smoothness in response for all listening positions. This would be the preferred location for placing the midranges in the IP.

For these preferred locations, there isn't much difference displayed in the angle of the midranges with respect to a mounting that is flush with the IP surface. The one exception is the Blue location for the driver's listening position. For this location, the surface orientation angle that is angled (-10º) toward the windshield has approximately 3dB more amplitude between 1.5k – 2.5k Hz.

There is more influence of the surface angle for other, less than ideal, locations, which in practice would be the more likely locations available, due to automotive packaging constraints and styling concerns.

CENTER TWEETER:

- For most listening positions, the Green location with a β angle or a Red location with a negative α angle are preferred.
- The more common and practical locations of the Pink and the Brown were the best solution for all listening positions with β angles.

What the simulations provide for both the outboard midranges and center tweeter then is the ability to make the decisions on the quality of a proposed location and angle with much the same confidence that we would have from in-vehicle measurements, which would only be available after the interior design was complete. This gives us the ability to modify early design decisions as much as possible for the most favorable results.

6. ACKNOWLEDGEMENTS

We would like to thank Alfred Svobodnik and Michal Bogdanski for their valuable assistance with this work.

7. REFERENCES

[1] R. Shively, J. Bailey, J. Halley, L. Kurandt, F. Malbos, G. Ruiz, A. Svobodnik, "Considerations for the Optimal Location and Boundary Effects for Loudspeakers in an Automotive Interior", Presented at the 128th Conv. of the AES, London, (2010 May), Preprint 8023.

[2] R.E. Shively, W.N. House, "Perceived Boundary Effects in an Automotive Vehicle Interior", Presented at the 100th Conv. of the AES, Copenhagen, (1996 May), Preprint 4245.

[3] R.E. Shively, "Automotive Audio: System Engineering", Presented to the AES Los Angeles Section, (1999 March).

[4] R.E. Shively "Automotive Audio Design (A Tutorial)", Presented at the 109th Conv. of the AES, Los Angeles, (2000 September), Preprint 5276

[5] A. Farina, "Simultaneous Measurement of Impulse Response and Distortion with a Swept-sine technique", Presented at the 108th AES Convention, Paris 2000, Preprint 5093

[6] S. Mueller, P. Massarani, "Transfer-Function Measurement with Sweeps", Director's cut, http://www.melaudia.net/zdoc/comparisonMesure.PDF, July 2009-07-21

8. APPENDIX (PRIOR ART)

8.1. General Instrument Panel Loudspeaker Location Guidelines (derived from Shively [2], [3], [4])

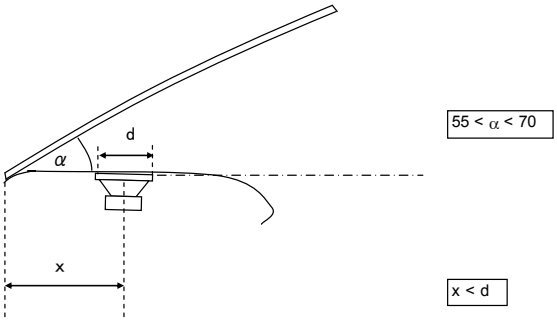

Figure 23. Windshield, Instrument Panel, Loudspeaker Example

8.1.1. Loudspeaker Location

For best sound quality, the distance (x) from the windshield baseline to the centerline of a loudspeaker located in the instrument panel should be at least one loudspeaker diameter (d).

8.1.2. Loudspeaker/Windshield Orientation Angle

For best sound quality, the angle (α) between the windshield and the loudspeaker-mounting plane should be between 55 º and 70 º.

If the angle is less than 55 º, the loudspeaker distance should move backward (away from the windshield) by a proportional amount or angled away from the windshield.

The larger the angle gets from 55 º toward 70 º, the more the loudspeaker should be angled toward the windshield. The loudspeaker should never be placed in a plane that is parallel with the windshield.

8.2. First Model: Cabin Geometry [1]

The geometry of the sedan vehicle is the basis for the acoustic mesh. No model update is applied. Characteristic boundary condition values are used instead.

The Acoustic mesh is derived from CATIA CAD model of the vehicle. Both the low-frequency model and the high-frequency model use the same CAD model as the starting point, but they require different meshes due to the different numerical schemes used. The low-frequency model covers frequency 100 - 1,000 Hz, while high-frequency model is used from 1,000 - 20,000 Hz.

8.3. Second Model [1]

The second model will perform a model update using measured data and the first model

8.3.1. In-Vehicle Measurements

Measurement Methods

As stated before, the lower frequency part of the frequency responses of the simulations is calculated by a wave expansion technique and the upper frequency part by a ray launching algorithm. The algorithms are based on different input data: the wave expansion method utilizes the frequency response and the ray launching method utilizes the impulse responses.

To guarantee a measurement with high accuracy for each simulation method an optimised measurement method is used. We consider that the loudspeaker and vehicle cabin embodiment is a time invariant system

with a transfer function. This transfer function is assumed to have a large linear part. The loudspeaker is excited at a low voltage level hence minimizing non-linear distortions.

For data utilized in conjunction with the high frequency simulation technique, measurements were performed with a logarithmic sweep as a test signal. This technique was introduced by Angelo Farina [5]. It provides the impulse response and is quite fast and robust.

For measurement data utilized in conjunction with low frequency simulation technique, a coherent stepped sine technique was used. This is a very robust technique as only noise of the currently measured frequency bin is involved in the measurement; see Mueller and Massarani [6]. During the measurement, tracking the nonlinear distortion and the SNR makes it simple for the user to figure out if a part of the measurement chain is not working well.

Sensors

The velocity of the cone is monitored with an accelerometer attached to the dustcap [Figures 24, 25]. Excitation voltage is probed at the driver's terminals. To scan the soundfield inside the cabin, a purposely built 12-microphones array and carrier embodiment was used [Figure 26]. The microphones used are small to minimize the impact on the soundfield and are close to omni-directional.

Positions of the microphones

Each microphone position inside the cabin is referenced to some characteristic points in the vehicle. Special attention is paid to the positions of the seats and the head-rests in order to replicate it inside the models.

SPL was measured in this vehicle at more 100 locations. Because of the massive number of measurement points inside the cabin, this data gathering exercise has been entitled the "100+ measurements". A sample of the measured frequency responses are depicted in Figure 27.

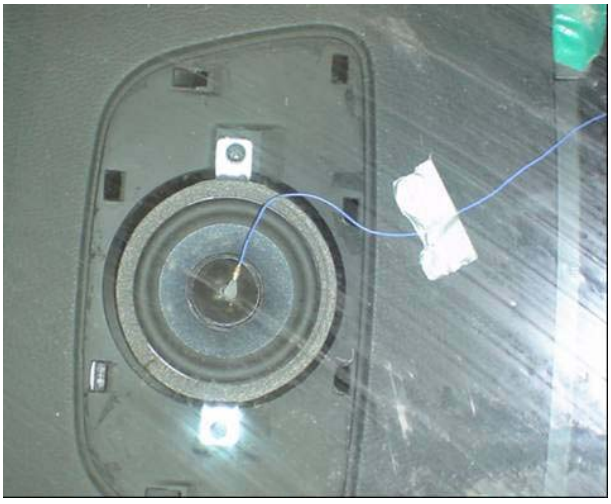

Figure 24. In-Vehicle Cone Velocity Measurements

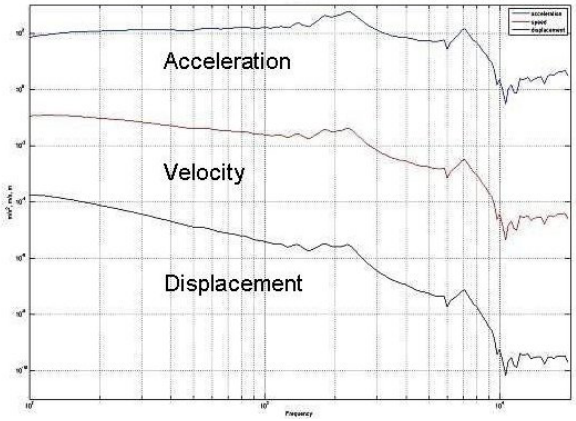

Figure 25. In-Vehicle Cone Acceleration, Velocity, and Displacement vs. Frequency

Figure 26. 12-microphones array and carrier embodiment.

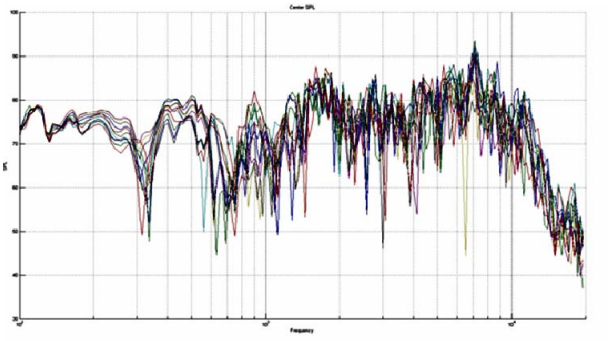

Figure 27. In-Vehicle SPL vs. Frequency from 100+ Microphone Measurements

8.4. Model Update

The model update procedure combines the 1st model results and 100+ measurements to determine appropriate acoustical properties of the interior and more accurate acoustical model of the cabin. The update procedure consists of an optimization loop. During the process, the model parameters are varied following a particular optimization scheme. The optimizer tries to minimize the error between the current model and a set of SPL measurements.

8.4.1. Error Calculation

Each SPL value is considered as a point in the Cartesian plane thus it's possible to calculate the aggregated normalized spatial distance between the target SPL and the calculated SPL. The target SPL (SPL_T) and calculated SPL (SPL_C) are defined as:

$$SPL_T = A_T(\cos(\alpha_T) + i\sin(\alpha_T))$$
$$SPLc = A_c(\cos(\alpha_c) + i\sin(\alpha_c))$$

where A_T and A_c are the absolute values of the target and calculated SPL and α_T and α_c are the angles of the pressure. The aggregated error E is defined as:

$$E = \frac{1}{N}\sqrt{\sum_{l=1}^{l=N}(A_{Tl}\cos\alpha_{Tl} - A_{cl}\cos\alpha_{cl})^2 + (A_{Tl}\sin\alpha_{Tl} - A_{cl}\sin\alpha_{cl})^2}$$

8.4.2. Updating Procedure

The updating procedure depends on a specified search range symmetric and centered to a complex material initial impedance value. Defining N and W the number of iterations and the impedance increment, the search range is equal to (2N+1)*W. The user has to specify an initial impedance value Z_{in}, thus the tested Z_t impedance values will be defined as:

$$Z_{ti} = Z_{in} + (i - N) * W \qquad \text{for } 0 \le i \le 2N$$

The vehicle cabin model is based on an impedance number N_Z, thus the updating procedure is launched $2*N_Z$. For each updating procedure, the impedance value used for the next iteration will correspond to the minimum error E.

To optimize the model update performances, the N iterations optimization process can be launched L times (L is the number of loops). For each loop, if the optimized solution corresponds to the lower (or upper) edge of the range, the search range needs to slide downwards (upwards) with an overlapping the two points, and the value W is not modified. If the optimized solution is not on the upper or lower edge, the W value is divided by the factor N.

For a model based on N_Z materials, L loops and N iterations, the model will be launched 2*(2N+1)*L*N times.

8.4.3. Process Description

The optimization process is structured in a way to enable it to be used by any of the numerical kernels proprietary to Harman International but also by any commercial solver. The input and output optimizer files are ASCII files. The optimization process procedure is described in Figure 28.

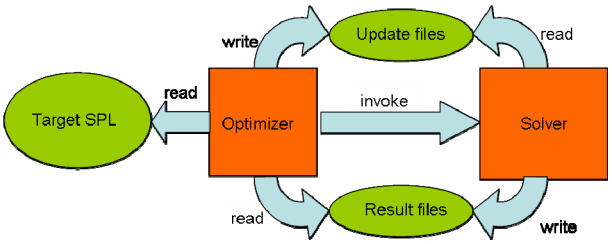

Figure 28. Model Update Optimization Process Procedure.

8.5. Introduction to Geometrical Acoustics

GA assumes a high mode density. A high modes density yields a high likelihood of a diffuse field. It is typically considered that this criterion is full-filled when at least three modes can be excited within their respective half-power points for any frequency under study. The threshold is known as the Schroeder frequency. Above this frequency, the energy propagates mainly along specular paths (i.e. like light) and then Snell's law applies. When hitting a surface, the energy is then: a) absorbed; b) reflected; and c) scattered.

There are several approaches in GA modeling. The historical approach is a fully deterministic calculation of all image sources relative to all planes in the geometry. This approach is called the Image Source Model (ISM). [Figure 29.] It is accurate but requires an exponentially increasing computation time as the reflection order increases. An alternate approach is a stochastic launch of rays or cones in all directions around the source. Rays/cones collected at the receiver location then define a valid path. [Figure 30.] This approach is efficient in terms of computation time but some paths might be missed. Different commercial packages are available using one of the two approaches, or combination of both. We are using a hybrid approach that combines ISM for first orders reflections; and Rays Launch for higher orders.

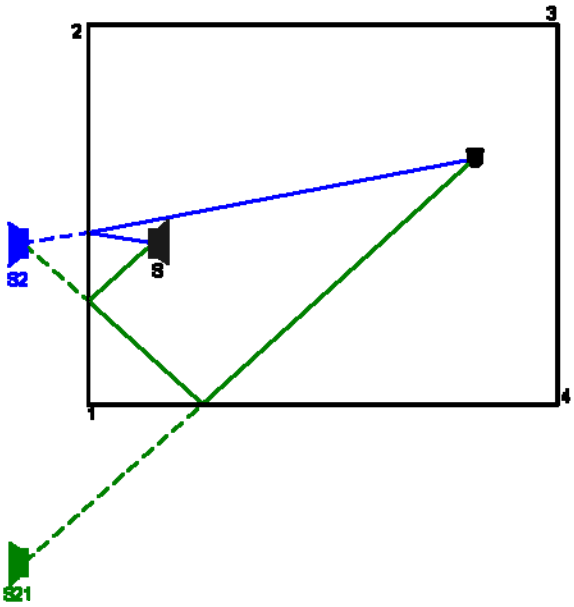

Figure 29. ISM Approach

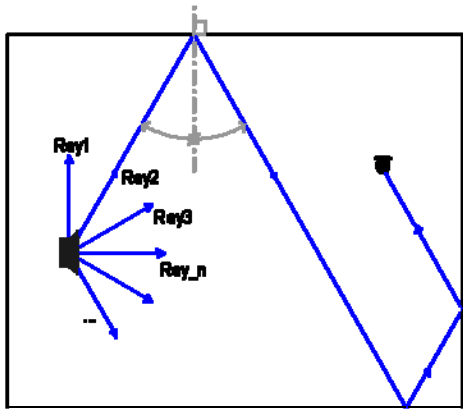

Figure 30. Random Rays Launch Approach

8.5.1. Inputs

Cabin geometry: The GA model mesh is an altered, simplified version of the low-frequency mesh featuring a relevant level of details. The mesh includes also the position of the different source(s) and receiver(s) as well as their orientation.

Source(s) characterization: The source is defined by its on-axis anechoic response and its directivity.

Material characterization: Each material type is defined by its absorption and scattering properties in each eight

octave bands from 125Hz to 16 kHz. These parameters are derived during the model update procedure.

8.5.2. The Model

The cabin interior modeled here has been meshed with 1,500+ elements. There are 18 receivers/microphones – i.e., an array of six microphones located at the front left, front right and rear left seat. The loudspeaker is defined as a source flush mounted on the instrument panel. The source is moved and angled to investigate different mounting options. Due to the volume of the cabin, we are investigating frequencies at 1 kHz and higher.